Identification of open quantum systems from observable time traces

Jun Zhang

Joint Institute of UM-SJTU and Key Laboratory of System Control and Information Processing (MOE), Shanghai Jiao Tong University, Shanghai, 200240, China

Mohan Sarovar[*]

Department of Scalable & Secure Systems Research, Sandia National Laboratories, Livermore, California 94550, USA

Estimating the parameters that dictate the dynamics of a quantum system is an important task for quantum information processing and quantum metrology, as well as fundamental physics. In this paper we develop a method for parameter estimation for Markovian open quantum systems using a temporal record of measurements on the system. The method is based on system realization theory and is a generalization of our previous work on identification of Hamiltonian parameters [Phys. Rev. Lett. **113**, 080401 (2014)].

PACS number(s): 03.65.Wj, 02.30.Yy, 03.67.−a

I. INTRODUCTION

Recent years have witnessed the rapid progress of quantum information processing technologies, including convincing demonstrations of a *quantum advantage* in several applications including communication and sensing. Such technologies require the precise fabrication and manipulation of quantum degrees of freedom, and as a result, much effort is invested into understanding and precisely identifying the quantum dynamics.

In Ref. [1] we developed a technique for identifying a parametrized Hamiltonian from time traces of expectation values of a small set of observables. This technique was recently experimentally demonstrated and validated in Ref. [2]. In the current paper we generalize this work to enable identification of parametrized open system evolution that can be described by a Lindblad master equation. This expands the applicability of this type of system identification approach that utilizes time traces of observables. As in Ref. [1] we consider only finite-dimensional systems, and assume that the system can be reliably prepared in a small number of initial states and possesses observables whose expectation value can be sampled over a period of time. Nuclear magnetic resonance [2,3] and ensembles of neutral atoms [4] are two typical examples of physical systems for which these assumptions are valid.

Our approach can be considered a generalization of traditional spectroscopic methods such as Ramsey interferometry in which spectral features of time-dependent data are used to infer values of underlying system parameters [3,5]. This inference is simple in the case of Ramsey or Rabi measurements where the relation between spectral features and the parameters is straightforward. In more complex situations, the relationship can be too complex to know *a priori*. Moreover, it may not even be known whether the measurements performed *can* identify a parameter of interest. Such complex situations beyond conventional spectroscopy can occur even in small systems such as a few atoms or spins. We develop a systematic way to perform parameter estimation in such complex situations, providing a criterion of whether the unknown parameters are estimable given the set of measurements available, and if so, prescribing a data-driven algorithm to identify them.

In addition to Ref. [1], previous studies that have examined this kind of *generalized spectroscopy* to estimate Hamiltonian or open system parameters from time traces include Refs. [6–18]. We draw particular attention to Ref. [15], in which the problem of identifying open quantum systems is studied in the same setting that we use. The solution constructed in that work is related to the one that we will present below in the sense that both consider observable time traces in the Laplace domain and attempt to solve equations encoding the relation between the unknown parameters and the measured signal. The principal difference is that, whereas in Ref. [15] the unknown parameters are expressed directly in terms of the measured signal, we use model realization theory to first construct a minimal model of the system from the measurements and then estimate the parameters from this minimal model.

The remainder of this paper is organized as follows: In Sec. II we formulate the system identification problem in the context of Markovian open quantum systems. Then in Sec. III we describe the identification algorithm based on model realization and highlight some of the distinctions between this algorithm and the corresponding algorithm for closed systems developed in Ref. [1]. We illustrate the open system algorithm with an example in Sec. IV, and in addition, we present several case studies in Appendix that exemplify the types of equation that must be solved in order to identify the parameters. Finally, in Sec. VI the paper is concluded with a discussion of results and future directions.

II. PROBLEM FORMULATION

The problem of interest is the identification of unknown parameters that dictate the dynamical behavior of a quantum system. The system state is represented by a density matrix $\rho \in \mathbb{C}^{N \times N}$, where $\rho^\dagger = \rho$, $\rho \geqslant 0$ (ρ is a positive semidefinite matrix), and tr $\rho = 1$. We assume that the system dynamics is governed by a quantum Markovian master equation in Lindblad form [19,20]:

$$\dot{\rho} = \mathcal{L}\rho \equiv \mathcal{L}_H\rho + \mathcal{L}_D\rho, \tag{1}$$

_____

[*]mnsarov@sandia.gov

where $\mathcal{L}_H$ is the generator of Hamiltonian dynamics

$$\mathcal{L}_H \rho = -i[H(\theta), \rho] \qquad (2)$$

with θ a vector of unknown parameters ($\hbar = 1$), and $\mathcal{L}_D$ represents a general Lindblad dissipative generator

$$\mathcal{L}_D \rho = \frac{1}{2} \sum_{j,k=1}^{N^2-1} g_{jk}([F_j, \rho F_k^\dagger] + [F_j \rho, F_k^\dagger]). \qquad (3)$$

Here $\{iF_k\}$ is an orthonormal basis for the Lie algebra $\mathfrak{su}(N)$, and the Hilbert-Schmidt inner product is defined as $\langle iF_m, iF_n \rangle \equiv \mathrm{tr}(F_m^\dagger F_n)$. Letting $\mathbf{G} = (g_{jk})_{j,k=1}^{N^2-1}$, we have that $\mathbf{G}^\dagger = \mathbf{G} \geqslant 0$ [20]. Expanding the Hamiltonian in this orthonormal basis, we obtain a parametrized Hamiltonian in the form

$$H(\theta) = \sum_{m=1}^{M} h_m(\theta) F_m, \qquad (4)$$

where $h_m = \mathrm{tr}(H F_m) \in \mathbb{R}$ are some known functions of θ. We take h_m as the unknown parameters from now on, since solving θ from h_m is an algebraic problem. The unknown parameters that we want to estimate are the Hamiltonian parameters h_m and the Lindblad coefficients g_{jk}.

First we define the structure constants $C_{jkl} \in \mathbb{C}$ of the Lie algebra $\mathfrak{su}(N)$ with respect to the orthonormal basis $\{iF_k\}$ through the commutator of basis elements:

$$[iF_j, iF_k] = \sum_{l=1}^{N^2-1} C_{jkl} iF_l. \qquad (5)$$

For future use we also define the constants $D_{jkl} \in \mathbb{C}$ through the anticommutator of basis elements [20]:

$$\{iF_j, iF_k\} = -\frac{2}{N}\delta_{jk}I + \sum_{l=1}^{N^2-1} D_{jkl} iF_l. \qquad (6)$$

The dynamics of the expectation value of an observable F_n, i.e., $x_n(t) = \mathrm{tr}\, F_n \rho(t)$, can be written as

$$\dot{x}_n(t) = \mathrm{tr}\, F_n[\mathcal{L}_H \rho(t) + \mathcal{L}_D \rho(t)]. \qquad (7)$$

From [1,19], we derive that

$$\dot{x}_n(t) = \sum_{p=1}^{N^2-1} (Q_{np} + R_{np})x_p(t) + b_n, \qquad (8)$$

where

$$Q_{np} = \sum_{m=1}^{M} C_{mnp} h_m,$$

$$R_{np} = -\frac{1}{4} \sum_{l,j,k=1}^{N^2-1} g_{jk}[C_{njl}(C_{klp} + D_{klp})$$

$$\qquad\qquad + C_{knl}(C_{ljp} + D_{ljp})], \qquad (9)$$

$$b_n = \frac{1}{N} \sum_{j,k=1}^{N^2-1} \mathrm{Im}(g_{jk}) C_{njk}.$$

Collecting the x_n in a vector $\mathbf{x} \in \mathbb{R}^{N^2-1}$, we obtain a linear differential equation describing the complete dynamics:

$$\dot{\mathbf{x}}(t) = \mathbf{A}\mathbf{x}(t) + \mathbf{b}, \quad x_n(0) = \mathrm{tr}\, F_n \rho(0), \qquad (10)$$

where the matrix $\mathbf{A} \in \mathbb{R}^{(N^2-1)\times(N^2-1)}$ has elements $A_{np} = Q_{np} + R_{np}$, and the vector $\mathbf{b} \in \mathbb{R}^{N^2-1}$ has elements b_n.

The vector $\mathbf{x}(t)$ is often called the *coherence vector*, and is a complete representation of the quantum state [19]. Equation (2) gives an explicit description of the quantum dynamics as a linear time-invariant (LTI) system, and hence it enables application of results from classical linear systems theory.

Next we turn to the observables being monitored. The measurement output consists of a vector of time-dependent observable expectation values:

$$\mathbf{y}(t) = [\langle O_1(t) \rangle, \langle O_2(t) \rangle, \dots]^\mathsf{T}. \qquad (11)$$

In most physical systems one has access to only a limited set of observables (e.g., local observables in a many-body system). However, as a result of the dynamics, it is possible that all the parameters defining Eq. (1) are imprinted in the time evolution of the monitored observables. This is the notion we wish to formalize and exploit. We begin by expanding each monitored observable O_i in the basis $\{iF_n\}$ of the Lie algebra $\mathfrak{su}(N)$, i.e., $O_i = \sum_{n=1}^{N^2-1} o_n^{(i)} F_n$. With this expansion we can define the output vector as

$$\mathbf{y}(t) = \mathbf{c}\mathbf{x}(t) \qquad (12)$$

with the ith row of the matrix $\mathbf{c}$ being the elements $o_n^{(i)}$. We also define the set $\mathcal{M} = \{F_{\nu_1}, F_{\nu_2}, \dots, F_{\nu_p}\}$, where $\boldsymbol{\nu}$ is a vector of length p, as the collection of unique basis elements that appear in the expansion of all the measured observables.

We want to use the dynamical equation governing the time evolution of only the observables being monitored to estimate the unknown parameters. It is possible that the evolution does not couple the elements in $\mathcal{M}$ to all elements of the basis. This is equivalent to $\mathbf{A}$ possessing block-diagonalizable structure and the elements of $\mathcal{M}$ being coupled only through a proper subblock. A constructive procedure to find the relevant basis elements that couple to the measured observables is the following generalization of the filtration procedure in geometric control theory [21]. First we define the adjoint generator of dynamics through $\dot{x}_n = \mathrm{tr}[F_n(\mathcal{L}\rho)] = \mathrm{tr}[(\mathcal{L}^\dagger F_n)\rho]$. Explicitly, $\mathcal{L}^\dagger X = \mathcal{L}_H^\dagger X + \mathcal{L}_D^\dagger X$, with

$$\mathcal{L}_H^\dagger X = -i[X, H(\theta)]$$

and

$$\mathcal{L}_D^\dagger X = \frac{1}{2} \sum_{j,k=1}^{N^2-1} g_{jk}([F_j, F_k^\dagger X] + [X F_j, F_k^\dagger]).$$

Then for the Lindblad dynamics in Eq. (1) we define an iterative procedure as

$$G_0 = \mathcal{M}, \quad G_i = \mathcal{L}^\dagger[G_{i-1}] \cup G_{i-1}, \qquad (13)$$

where

$$\mathcal{L}^\dagger[G_{i-1}] = \{F_j : \mathrm{tr}(F_j^\dagger \mathcal{L}^\dagger g) \neq 0 \quad \text{where} \quad g \in G_{i-1}\}.$$

That is, at each iteration we compute the adjoint evolution of each of the elements of G_{i-1}, and if the result has nonzero inner product with a basis element not already in G_{i-1}, this basis element is added to G_i. Since the dynamical system is finite dimensional, this iteration will saturate at a maximal set $\bar{G}$ after finite steps, and we refer to this set as the *accessible set*. Now writing all the x_k with $F_k \in \bar{G}$ in a vector $\mathbf{x}_a$ of dimension $K \leqslant N^2 - 1$, the dynamics for this vector is given by

$$\frac{d}{dt}\mathbf{x}_a = \tilde{\mathbf{A}}\mathbf{x}_a + \tilde{\mathbf{b}}, \tag{14}$$

$$\mathbf{y}(t) = \tilde{\mathbf{c}}\mathbf{x}_a(t), \tag{15}$$

where $\tilde{\mathbf{A}}$ is a $K \times K$ submatrix of $\mathbf{A}$, $\tilde{\mathbf{b}}$ is a $K \times 1$ subvector of $\mathbf{b}$, and $\tilde{\mathbf{c}}$ is a $p \times K$ submatrix of $\mathbf{c}$; i.e., all contain only the elements necessary to describe the evolution of the subset of observable averages collected in $\mathbf{x}_a$ and how these define the measurement traces.

Finally, we assume that the system is prepared in a fixed, known initial state $\mathbf{x}(0)$, and the corresponding initial state for Eq. (14) is $\mathbf{x}_a(0)$.

III. IDENTIFICATION ALGORITHM

Suppose that we can measure the expectation values of some observables in $\mathcal{M}$ at regular time instants $j\Delta t$, where Δt is the sampling period. Denote the measured expectation values of the observables as $\{\mathbf{y}(j\Delta t)\}$,[1] which is the output of the following discretized form of Eq. (14):

$$\mathbf{x}_a(j+1) = \tilde{\mathbf{A}}_d \left[\mathbf{x}_a(j) + \int_{j\Delta t}^{(j+1)\Delta t} d\tau e^{-\tilde{\mathbf{A}}\tau}\tilde{\mathbf{b}} \right],$$
$$\mathbf{y}(j) = \tilde{\mathbf{c}}\mathbf{x}_a(j), \tag{16}$$

where $\tilde{\mathbf{A}}_d = e^{\tilde{\mathbf{A}}\Delta t}$, and for brevity of notation we use $\mathbf{x}_a(j) \equiv \mathbf{x}_a(j\Delta t)$ and $\mathbf{y}(j) \equiv \mathbf{y}(j\Delta t)$.

Equation (16) defines a discrete-time LTI system, and we will now use invariants of different realizations of an LTI system to identify the unknown Hamiltonian and Lindblad parameters that generate the dynamics. To this end, we need to construct a realization from the measurement time traces. There are many methods for constructing a realization of a linear dynamical system from input-output data in linear systems theory [22]. In [1], we presented and utilized a method called the eigenstate realization algorithm (ERA) [23] for identifying Hamiltonian dynamics, and in the following we show that this method can be used in this case of open-system dynamics in Lindblad form also. For completeness, we include the specification of the ERA here.

A. Eigenstate realization algorithm

The first stage of the estimation algorithm is to construct a minimal realization of the system based on input-output information. This is achieved by the ERA in three steps as follows.

Step 1. Collect the measured data into an $rp \times s$ matrix (generalized Hankel matrix) as

$$\mathbf{H}_{rs}(k) =$$

$$\begin{bmatrix} \mathbf{y}(k) & \mathbf{y}(k+t_1) & \cdots & \mathbf{y}(k+t_{s-1}) \\ \mathbf{y}(j_1+k) & \mathbf{y}(j_1+k+t_1) & \cdots & \mathbf{y}(j_1+k+t_{s-1}) \\ \vdots & \vdots & & \vdots \\ \mathbf{y}(j_{r-1}+k) & \mathbf{y}(j_{r-1}+k+t_1) & \cdots & \mathbf{y}(j_{r-1}+k+t_{s-1}) \end{bmatrix}$$

with arbitrary integers j_i ($i = 1, \ldots, r-1$) and t_l ($l = 1, \ldots, s-1$).

Step 2. Find the singular value decomposition of $\mathbf{H}_{rs}(0)$ as

$$\mathbf{H}_{rs}(0) = P \begin{bmatrix} \Sigma & 0 \\ 0 & 0 \end{bmatrix} Q^{\mathsf{T}} = [P_1 \quad P_2] \begin{bmatrix} \Sigma & 0 \\ 0 & 0 \end{bmatrix} \begin{bmatrix} Q_1^{\mathsf{T}} \\ Q_2^{\mathsf{T}} \end{bmatrix},$$

where $P \in \mathbb{R}^{rp \times rp}$ and $Q \in \mathbb{R}^{s \times s}$ are both orthonormal, and Σ is a diagonal matrix with the nonzero singular values of $\mathbf{H}_{rs}(0)$ determined up to numerical accuracy ϵ, i.e., $\Sigma_{ii} > \epsilon$ for all $i \leqslant n_\Sigma$ where n_Σ is the dimension of Σ. The matrices P_1, P_2, Q_1, and Q_2 are partitions with compatible dimensions. When the measurement time traces are noisy, determining the cutoff parameter ϵ (and hence n_Σ) can be difficult since the noise can lead to nondecaying singular values. In this case, one can choose n_Σ by demanding that the realization produced by the ERA is of the correct order. We will return to this issue when we specify how the ERA realization will be used [see discussion after Eq. (18)].

Step 3. Form a realization of the system (16) as $\hat{\mathbf{A}}_d = \Sigma^{-1/2}P_1^{\mathsf{T}}\mathbf{H}_{rs}(1)Q_1\Sigma^{-1/2}$, $\hat{\mathbf{c}} = \mathsf{E}_p^{\mathsf{T}}P_1\Sigma^{1/2}$, and $\hat{\mathbf{x}}(0) \equiv \Sigma^{1/2}Q_1^{\mathsf{T}}e_1$, where $\mathsf{E}_p^{\mathsf{T}} = [\mathbf{I}_p, 0_p, \ldots, 0_p]$ and e_1 is the first column of $\mathbf{I}_s$. The triple $(\hat{\mathbf{A}}_d, \hat{\mathbf{c}}, \hat{\mathbf{x}}(0))$ forms a realization of Eq. (16), and since the output data are an invariant of realizations, this triple generates the same output as the original system:

$$\mathbf{y}(j) = \hat{\mathbf{c}}\hat{\mathbf{A}}_d^j\hat{\mathbf{x}}(0) \quad \text{for all} \quad j \geqslant 0. \tag{17}$$

Note that, although the original system response is composed of a response to a nonzero initial state and a response to the forcing vector $\tilde{\mathbf{b}}$ [i.e., Eq. (16)], the ERA realization is composed of only an initial-state response. This is because at the level of input-output realizations it is not possible to distinguish between the response to initial states and the response to forcing inputs, and therefore the ERA lumps all responses into one type.

This completes the specification of the ERA algorithm. It results in a realization of the discrete-time dynamical system (16) in the form of the triple $(\hat{\mathbf{A}}_d, \hat{\mathbf{c}}, \hat{\mathbf{x}}(0))$.

We note that the measurement results do not have to be uniform in Step 1 of the algorithm; in particular, if it is known that some measurement results are particularly noisy or corrupted, those data points can be discarded by choosing appropriate integers j_i ($i = 1, \ldots, r-1$) and t_l ($l = 1, \ldots, s-1$). This data filtering can reduce the estimation error caused by measurement noise and outliers.

B. Estimation algorithm

In order to estimate the parameters in the original dynamical system, we now convert the discrete-time LTI system

---

[1]Note that these expectation values may have to be collected from averaging measurements on several runs of the experiment under the same initial state.

realization obtained from the ERA, $(\hat{\mathbf{A}}_d, \hat{\mathbf{c}}, \hat{\mathbf{x}}(0))$, to a continuous-time realization, by letting $\hat{\mathbf{A}} \equiv \log \hat{\mathbf{A}}_d / \Delta t$, where the logarithm in this definition is the principal branch of the natural logarithm. The accurate conversion from a discrete-time system to a continuous-time system relies on the sampling time Δt being sufficiently small to capture all continuous-time dynamics. For the Hamiltonian system identification case we were able to specify conditions on the sampling time based on the Shannon-Nyquist criterion, since in this case the output time traces $\mathbf{y}(t)$ are guaranteed to be band limited [1]. However, there is no such guarantee in the Markovian open system case since now the time traces are generally decaying oscillations, or *time-limited* sigmals. Therefore, we do not currently have conditions on the sampling time for this conversion to accurately provide a continuous-time realization (i.e., to avoid aliasing effects), but note that one can generally estimate a valid sampling time from knowledge of the intrinsic frequencies in the system. In engineering, it is typical practice to sample such time-limited signals at six or eight times the fastest frequency in the signal [24], and such a heuristic suffices in our setting as well, as the example in Sec. IV and the case studies in the Appendix bear out. Additionally, we note that, although the Shannon-Nyquist criterion enables a formal specification of the minimum sampling time in the Hamiltonian estimation scenario, to apply it requires some knowledge of the system's spectrum. In the absence of this knowledge, the situation is the same in the closed- and open-system cases: one needs to estimate a valid sampling time and possibly also try multiple sampling times.

Now, to estimate the unknown parameters, we use the fact that the system input-output relations are invariants of different realizations. We work in the Laplace domain in the following in order to form algebraic equations for the unknown parameters. By equating the Laplace transform of the outputs of the original system and the ERA realization we get

$$\tilde{\mathbf{c}}(s\mathbf{I} - \tilde{\mathbf{A}})^{-1} \left(\mathbf{x}_a(0) + \frac{\tilde{\mathbf{b}}}{s} \right) = \hat{\mathbf{c}}(s\mathbf{I} - \hat{\mathbf{A}})^{-1} \hat{\mathbf{x}}(0). \qquad (18)$$

This equation relates the unknown parameters to the measured data through the ERA realization. Explicitly, the right-hand side of Eq. (18) is completely determined by the measured data, and the left-hand side is in terms of the Hamiltonian parameters h_m and Lindblad coefficients g_{jk}. The resolvent expressions on the right- and left-hand sides of Eq. (18), $(s\mathbf{I} - \tilde{\mathbf{A}})^{-1}$ and $(s\mathbf{I} - \hat{\mathbf{A}})^{-1}$, can be computed symbolically, or alternatively the expressions can be expanded in powers of s, and the coefficients in this expansion can be equated to yield polynomial equations for the unknown parameters. Solution of these multivariate polynomial equations leads to the identification of g_m and a_{jk}. In the case studies encountered in the Appendix we are able to express the resolvents exactly by computing the matrix inverses symbolically, but one may need to resort to the expansion in s in more complicated cases. We discuss this issue further in Sec. VI.

Note that n_Σ in Step 2 of the ERA dictates the maximum order of the polynomial on the right-hand side of Eq. (18). This suggests that we should choose n_Σ to be of the order of the denominator polynomial in the left-hand side of Eq. (18), which can be calculated from symbolic computations and

obtained as an irreducible rational function. This choice coincides with the rank of $\mathbf{H}_{rs}(0)$ when there is no noise in the measurement time traces.

We highlight a crucial difference here between parameter estimation in the closed system and Markovian open-system scenarios. For the former, $\mathbf{b} = \mathbf{0}$, and if the triple $(\tilde{\mathbf{A}}, \tilde{\mathbf{c}}, \mathbf{x}_a(0))$ forms a minimal realization (i.e., is controllable and observable), then the Laplace transform on the left-hand side of Eq. (18) is guaranteed to have a canonical form as a ratio of polynomials $Q(s)/P(s)$ [22], with

$$\begin{aligned} P(s) &= \det(s\mathbf{I} - \tilde{\mathbf{A}}), \\ Q(s) &= \det \left(s \begin{bmatrix} \mathbf{I} & \mathbf{0} \\ \mathbf{0} & \mathbf{0} \end{bmatrix} - \begin{bmatrix} \tilde{\mathbf{A}} & \mathbf{x}_a(0) \\ \tilde{\mathbf{c}} & \mathbf{0} \end{bmatrix} \right). \end{aligned} \qquad (19)$$

Having this form enabled us in Ref. [1] to avoid explicitly computing the inverse $(s\mathbf{I} - \tilde{\mathbf{A}})^{-1}$ or its expansion in a power series. These are both computationally intensive to compute since the matrix $\tilde{\mathbf{A}}$ is a symbolic matrix containing the unknown parameters. However, in the open-system case, where the left-hand side of Eq. (18) has no known canonical form, one cannot avoid performing this symbolic inverse or power series computation. This is a critical difference in computational difficulty between the closed- and open-system parameter identification problems.

We note that by converting back into the continuous-time domain and formulating the Laplace transform relation in Eq. (18), we have converted the problem of estimating parameters to one of solving polynomial equations. This is in contrast to direct estimation of parameters using Eq. (17), which would involve solving transcendental equations for the unknown parameters. This simplification of the equations relating the unknown parameters to the measured data is one of the primary advantages of our approach.

We conclude with two further comments on the above estimation algorithm:

(1) The initial state may have to be chosen carefully. For example, if $\mathbf{x}_a$ is zero or an eigenvector of $\tilde{\mathbf{A}}$, it leads to no sensitivity in the output to any of the unknown parameters. Care must be taken to avoid such degenerate cases. In fact, running the algorithm with multiple initial states leads to more polynomial equations of low order and thus can help to solve for the unknown parameters more efficiently.

(2) This system identification algorithm can result in multiple estimates of the unknown parameters, all of which satisfy the input-output relations captured by Eq. (18). This is because several Markovian generators can generate the same map between an input state and the measurement time trace, and hence are equivalent from an input-output perspective [25]. When the algorithm results in multiple parameter estimates, one has to appeal to prior information, or add resources such as additional input states or observable time traces in order to uniquely specify a parameter set.

The following section explicitly demonstrates the algorithm developed above and the Appendix presents additional case studies.

IV. DISSIPATIVE ENERGY TRANSFER

In this section we apply the estimation algorithm developed above to a physically relevant example: energy transfer

between two qubits at finite temperature. The qubits could represent the relevant energy levels of an atomic or molecular system, or a spin-$\frac{1}{2}$ system. The Markovian master equation for the dynamics takes the form

$$
\frac{d\rho}{dt} = -i[H,\rho] + \sum_{k=1}^{2} \frac{\gamma_k}{2}\left(\sigma_z^k \rho \sigma_z^k - \rho\right)
$$
$$
+ \sum_{k=1}^{2} 2g_k^-\left(\sigma_-^k \rho \sigma_+^k - \frac{1}{2}\sigma_+^k\sigma_-^k\rho - \frac{1}{2}\rho\sigma_+^k\sigma_-^k\right)
$$
$$
+ 2g_k^+\left(\sigma_+^k \rho \sigma_-^k - \frac{1}{2}\sigma_-^k\sigma_+^k\rho - \frac{1}{2}\rho\sigma_-^k\sigma_+^k\right), \quad (20)
$$

where the Hamiltonian for the system is given by

$$
H = \frac{\omega_1}{2}\sigma_z^1 + \frac{\omega_2}{2}\sigma_z^2 + \delta_1(\sigma_+^1\sigma_-^2 + \sigma_-^1\sigma_+^2). \quad (21)
$$

This is a model for two possibly detuned qubits with coherent energy transfer dynamics, independent dephasing,

and incoherent excitation and relaxation. The rates of excitation and relaxation (g_k^+ and g_k^-) are functions of the temperature of the environment of the qubits [26]. There are nine parameters that dictate the dynamics in this model: $\theta = (\omega_1,\omega_2,\delta_1,\gamma_1,\gamma_2,g_1^+,g_1^-,g_2^+,g_2^-)$. For convenience, we define

$$
\nu_1 = g_1^+ + g_1^-, \quad \mu_1 = g_1^+ - g_1^-,
$$
$$
\nu_2 = g_2^+ + g_2^-, \quad \mu_2 = g_2^+ - g_2^-. \quad (22)
$$

Assume that the observable being measured is $\bar{z}_1(t) \equiv \langle\sigma_z^1(t)\rangle$, or $\bar{z}_2(t) \equiv \langle\sigma_z^2(t)\rangle$, or both, since we will be interested in exploring the benefits of measuring multiple observables. The state vector determined by the accessible set is the same regardless of whether one or both of those observables are measured and is explicitly specified by $\mathbf{x}_a = [\langle\sigma_z^1\rangle, \langle\sigma_z^2\rangle, \langle\sigma_x^1\sigma_x^2\rangle, \langle\sigma_x^1\sigma_y^2\rangle, \langle\sigma_y^1\sigma_x^2\rangle, \langle\sigma_y^1\sigma_y^2\rangle]$, whereas the dynamics of $\mathbf{x}_a$ is determined by Eq. (14) with

$$
\tilde{\mathbf{A}} = \begin{bmatrix}
-2\nu_1 & 0 & 0 & \delta_1 & -\delta_1 & 0 \\
0 & -2\nu_2 & 0 & -\delta_1 & \delta_1 & 0 \\
0 & 0 & -\nu_s - \gamma_s & \omega_2 & \omega_1 & 0 \\
-\delta_1 & \delta_1 & -\omega_2 & -\nu_s - \gamma_s & 0 & \omega_1 \\
\delta_1 & -\delta_1 & -\omega_1 & 0 & -\nu_s - \gamma_s & \omega_2 \\
0 & 0 & 0 & -\omega_1 & -\omega_2 & -\nu_s - \gamma_s
\end{bmatrix},
$$
$$
\tilde{\mathbf{b}} = [\mu_1, \quad \mu_2, \quad 0, \quad 0, \quad 0, \quad 0]^{\mathsf{T}},
$$

where $\nu_s = \nu_1 + \nu_2$ and $\gamma_s = \gamma_1 + \gamma_2$. The matrix defining the output depends on which observable is being monitored and is given by

$$
\langle\sigma_z^1\rangle: \quad \tilde{\mathbf{c}}_{z_1} = [1,0,0,0,0,0], \quad \text{or}
$$
$$
\langle\sigma_z^2\rangle: \quad \tilde{\mathbf{c}}_{z_2} = [0,1,0,0,0,0], \quad (23)
$$

or the concatenation of these two row vectors into a 2×6 matrix $\tilde{\mathbf{c}}_{z_1 z_2}$ if both observables are being monitored.

Letting the initial state be $|\psi_1(0)\rangle = |0\rangle \otimes (|0\rangle + |1\rangle)/\sqrt{2}$, we have that

$$
\mathbf{x}_a(0) = [1, \quad 0, \quad 0, \quad 0, \quad 0, \quad 0]^{\mathsf{T}}. \quad (24)
$$

Since the matrix $\tilde{\mathbf{A}}$ is small, we can symbolically calculate the resolvents in Eq. (18), to obtain the Laplace transform of the two possible measurement traces $\bar{z}_1(t)$ or $\bar{z}_2(t)$:

$$
\bar{Z}_1(s) = \tilde{\mathbf{c}}_{z_1}(s\mathbf{I} - \tilde{\mathbf{A}})^{-1}\mathbf{x}_a(0) + \tilde{\mathbf{c}}_{z_1}(s\mathbf{I} - \tilde{\mathbf{A}})^{-1}\tilde{\mathbf{b}}/s
$$
$$
= \frac{s^4 + q_3 s^3 + q_2 s^2 + q_1 s + q_0}{s^5 + p_4 s^4 + p_3 s^3 + p_2 s^2 + p_1 s} \quad (25)
$$

with

$$
q_3 = \mu_1 + 2\nu_1 + 4\nu_2 + 2\gamma_s,
$$
$$
q_2 = 2\delta_1^2 + \nu_1^2 + 6\nu_1\nu_2 + 2\nu_1\gamma_s + 2\mu_1\nu_1 + 5\nu_2^2 + 6\nu_2\gamma_s
$$
$$
+ 4\mu_1\nu_2 + \gamma_s^2 + 2\mu_1\gamma_s + \omega_d^2,
$$
$$
q_1 = 2\delta_1^2\mu_1 + 2\delta_1^2\mu_2 + 2\delta_1^2\nu_1 + 2\delta_1^2\nu_2 + 2\delta_1^2\gamma_s + \mu_1\nu_1^2
$$
$$
+ 5\mu_1\nu_2^2 + 4\nu_1\nu_2^2 + 2\nu_1^2\nu_2 + \mu_1\gamma_s^2 + 2\nu_2\gamma_s^2 + 4\nu_2^2\gamma_s
$$

$$
+ \mu_1\omega_d^2 + 2\nu_2\omega_d^2 + 2\nu_2^3 + 6\mu_1\nu_1\nu_2 + 2\mu_1\nu_1\gamma_s
$$
$$
+ 6\mu_1\nu_2\gamma_s + 4\nu_1\nu_2\gamma_s,
$$
$$
q_0 = 2\mu_1\nu_2^3 + 2\delta_1^2\mu_1\gamma_s + 2\delta_1^2\mu_2\gamma_s + 4\mu_1\nu_1\nu_2^2 + 2\mu_1\nu_1^2\nu_2
$$
$$
+ 2\mu_1\nu_2\gamma_s^2 + 4\mu_1\nu_2^2\gamma_s + 2\mu_1\nu_2\omega_d^2 + 2\delta_1^2\mu_1\nu_1
$$
$$
+ 2\delta_1^2\mu_1\nu_2 + 2\delta_1^2\mu_2\nu_1 + 2\delta_1^2\mu_2\nu_2 + 4\mu_1\nu_1\nu_2\gamma_s, \quad (26)
$$

and

$$
p_4 = 4\nu_1 + 4\nu_2 + 2\gamma_s,
$$
$$
p_3 = 4\delta_1^2 + 5\nu_1^2 + 14\nu_1\nu_2 + 6\nu_1\gamma_s + 5\nu_2^2 + 6\nu_2\gamma_s
$$
$$
+ \gamma_s^2 + \omega_d^2,
$$
$$
p_2 = 8\delta_1^2\nu_1 + 8\delta_1^2\nu_2 + 4\delta_1^2\gamma_s + 2\nu_1^3 + 14\nu_1^2\nu_2 + 4\nu_1^2\gamma_s
$$
$$
+ 14\nu_1\nu_2^2 + 16\nu_1\nu_2\gamma_s + 2\nu_1\gamma_s^2 + 2\nu_1\omega_d^2 + 2\nu_2^3 \quad (27)
$$
$$
+ 4\nu_2^2\gamma_s + 2\nu_2\gamma_s^2 + 2\nu_2\omega_d^2,
$$
$$
p_1 = 4\delta_1^2\nu_1^2 + 8\delta_1^2\nu_1\nu_2 + 4\delta_1^2\nu_1\gamma_s + 4\delta_1^2\nu_2^2 + 4\delta_1^2\nu_2\gamma_s
$$
$$
+ 4\nu_1^3\nu_2 + 8\nu_1^2\nu_2^2 + 8\nu_1^2\nu_2\gamma_s + 4\nu_1\nu_2^3 + 8\nu_1\nu_2^2\gamma_s
$$
$$
+ 4\nu_1\nu_2\gamma_s^2 + 4\nu_1\nu_2\omega_d^2,
$$

where $\omega_d = \omega_1 - \omega_2$. And

$$
\bar{Z}_2(s) = \tilde{\mathbf{c}}_{z_2}(s\mathbf{I} - \tilde{\mathbf{A}})^{-1}\mathbf{x}_a(0) + \tilde{\mathbf{c}}_{z_2}(s\mathbf{I} - \tilde{\mathbf{A}})^{-1}\tilde{\mathbf{b}}/s
$$
$$
= \frac{r_3 s^3 + r_2 s^2 + r_1 s + r_0}{s^5 + p_4 s^4 + p_3 s^3 + p_2 s^2 + p_1 s}, \quad (28)
$$

with

$$r_3 = \mu_2,$$

$$r_2 = 2\delta_1^2 + 4\mu_2\nu_1 + 2\mu_2\nu_2 + 2\mu_2\gamma_s,$$

$$\begin{aligned} r_1 = {} & 2\delta_1^2\mu_1 + 2\delta_1^2\mu_2 + 2\delta_1^2\nu_1 + 2\delta_1^2\nu_2 + 2\delta_1^2\gamma_s + 5\mu_2\nu_1^2 \\ & + \mu_2\nu_2^2 + \mu_2\gamma_s^2 + \mu_2\omega_d^2 + 6\mu_2\nu_1\nu_2 + 6\mu_2\nu_1\gamma_s \\ & + 2\mu_2\nu_2\gamma_s, \end{aligned}$$

$$\begin{aligned} r_0 = {} & 2\mu_2\nu_1^3 + 2\delta_1^2\mu_1\gamma_s + 2\delta_1^2\mu_2\gamma_s + 2\mu_2\nu_1\nu_2^2 + 4\mu_2\nu_1^2\nu_2 \\ & + 2\mu_2\nu_1\gamma_s^2 + 4\mu_2\nu_1^2\gamma_s + 2\mu_2\nu_1\omega_d^2 + 2\delta_1^2\mu_1\nu_1 \\ & + 2\delta_1^2\mu_1\nu_2 + 2\delta_1^2\mu_2\nu_1 + 2\delta_1^2\mu_2\nu_2 + 4\mu_2\nu_1\nu_2\gamma_s \end{aligned}$$

(29)

and p_i defined as in Eq. (27).

It is clear from these expressions that we can identify ν_i and μ_i, which then allows identification of g_i^+ and g_i^-. At the same time, note that only the linear combinations $\gamma_s = \gamma_1 + \gamma_2$ and $\omega_d = \omega_1 - \omega_2$ occur in the above equations but not the individual parameters γ_i and ω_i ($i = 1, 2$). This implies that only these linear combinations can be determined from the measurements and the initial state, but not the individual parameters that enter them. These linear combinations describe the energy difference between the qubits and the dephasing-induced broadening of this energy difference. The physical observables encoding the average population of the excited state of either qubit allow only determination of these collective (in the case of γ_s) or relative (in the case of ω_d) properties of the system. Furthermore, another restriction that we can immediately observe is that only even powers of δ_1 and ω_d occur in all of the polynomials above, and therefore we expect to determine these parameters only up to a sign difference. The signs of these parameters are not estimable by the local measurements we have chosen, and prior knowledge or additional initial states or measurements are necessary to identify these signs.

Before we present the results of the estimation simulation, we outline four possible modes of estimation that could be performed given that there are two possible observables:

(1) In mode 1, only the measurement trace $\bar{z}_1(t)$ is used to construct the Hankel matrix and system realization ($\tilde{\mathbf{c}} = \tilde{\mathbf{c}}_{z_1}$), and the polynomial system used to solve for the unknown parameters is constructed using only $\bar{Z}_1(s)$.

(2) In mode 2, only the measurement trace $\bar{z}_2(t)$ is used to construct the Hankel matrix and system realization ($\tilde{\mathbf{c}} = \tilde{\mathbf{c}}_{z_2}$), and the polynomial system used to solve for the unknown parameters is constructed using only $\bar{Z}_2(s)$.

(3) In mode 3, the measurement traces $\bar{z}_1(t)$ and $\bar{z}_2(t)$ are used to construct the Hankel matrix and system realization ($\tilde{\mathbf{c}} = \tilde{\mathbf{c}}_{z_1 z_2}$), and the polynomial system used to solve for the unknown parameters is constructed using only $\bar{Z}_1(s)$.

(4) In mode 4, the measurement traces $\bar{z}_1(t)$ and $\bar{z}_2(t)$ are used to construct the Hankel matrix and system realization ($\tilde{\mathbf{c}} = \tilde{\mathbf{c}}_{z_1 z_2}$), and the polynomial system used to solve for the unknown parameters is constructed using only $\bar{Z}_2(s)$.

Obviously, modes 1 and 2 are practically more attractive since they involve collecting only one observable's time trace. However, there may be a benefit to considering modes 3 and 4 since in these modes of estimation one is providing the algorithm with more data with which to construct the
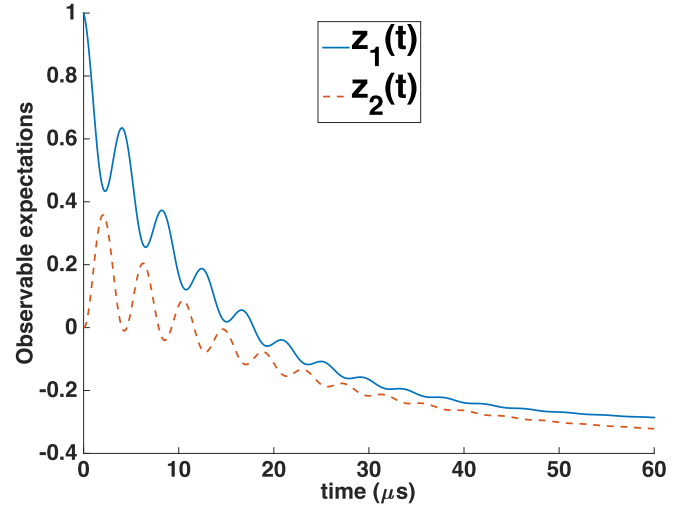

FIG. 1. (Color online) Measurement time traces of $\langle\sigma_z^1(t)\rangle$ and $\langle\sigma_z^2(t)\rangle$ for the energy transfer example presented in Sec. IV. The initial-state and system parameters are specified in the text.

realization (although the accessible vector does not change, and so some of these additional data are redundant). One could also imagine a fifth mode where one uses the measurement traces $\bar{z}_1(t)$ and $\bar{z}_2(t)$ to construct the Hankel matrix and system realization ($\tilde{\mathbf{c}} = \tilde{\mathbf{c}}_{z_1 z_2}$), and then constructs the polynomial system from the definitions of both $\bar{Z}_1(s)$ and $\bar{Z}_2(s)$, i.e., some polynomial equations from the definition of the coefficients in $\bar{Z}_1(s)$ and some from the definition of the coefficients in $\bar{Z}_2(s)$. For our example, where the number of parameters is small enough such that one can get enough equations from using the definition of just one of the Laplace transforms, we did not find any advantage to using this fifth mode of estimation, and so do not investigate it further.

To illustrate the algorithm we fix the nominal parameters of the system as $\omega_1 = 1.3$ MHz, $\omega_2 = 2.4$ MHz, $\delta_1 = 0.5$ MHz, $\gamma_1 = 0.03$ MHz, $\gamma_2 = 0.035$ MHz, $g_i^+ = 0.02\bar{n}(\omega_i)$ MHz, $g_i^- = 0.02[\bar{n}(\omega_i) + 1]$ MHz, with

$$\bar{n}(\omega) = \frac{1}{e^{\omega/k_B T} - 1}$$

being the Bose-Einstein distribution at temperature T. In the following we fix the temperature at $k_B T = 0.8\omega_1$. For a system with these parameters, we generate a time trace of $\bar{z}_1(t)$ and $\bar{z}_2(t)$ from $t = 0$ to $t = t_f \equiv 60$ μs, with $\Delta t = 0.01$ μs. The resulting time traces are shown in Fig. 1. We form the Hankel matrix using either one or both of these time traces, depending on the mode of estimation, with $t_i = j_i = 1$ (i.e., using every data point), and $r = s = \frac{t_f/\Delta t}{2}$. The ERA realization of the discrete-time system is formed with $n_\Sigma = \text{rank}[\mathbf{H}_{rs}(0)]$, and the corresponding continuous-time system is formed using the prescription given in Sec. III B. Finally, the Laplace transform expression on the right-hand side of Eq. (18) is computed to obtain[2]

$$\bar{Z}_1^{est}(s) = \frac{s^4 + 0.2702s^3 + 1.7302s^2 + 0.072s - 0.0034}{s^5 + 0.3624s^4 + 2.2569s^3 + 0.3243s^2 + 0.011s}$$

---

[2]We used the MATLAB Control System Toolbox function TF in order to obtain these Laplace transforms.

TABLE I. Estimates derived from noiseless measurement traces. The modes of estimation (modes 1 and 2) are explained in the text.

Parameter	ω_d	δ_1	ν_1	ν_2	μ_1	μ_2	γ_s
Nominal value	-1.1	0.5	0.0361	0.022	-0.02	-0.0176	0.065
Mode 1	±1.0973	±0.5029	0.0677	-0.0096	0.0432	-0.0815	0.065
	±1.1	±0.5	0.0361	0.022	-0.02	-0.0176	0.065
Mode 2	±1.1	±0.5	0.0361	0.022	-0.02	-0.0176	0.065

and

$$\bar{Z}_2^{est}(s) = \frac{-0.0176s^3 + 0.4944s^2 + 0.0209s - 0.0039}{s^5 + 0.3624s^4 + 2.2569s^3 + 0.3243s^2 + 0.011s}.$$

Combining these expressions with the corresponding Laplace transforms Eqs. (25) and (28), we obtain a system of polynomial equations for the unknown parameters (we can choose the seven simplest equations since there are seven unknown parameters). We solved these equations using PHCLAB, the MATLAB interface to the PHCPACK libraries for solving polynomial systems [27].

Table I shows the results of solving for the parameters when the measurements are noiseless. We found no difference between modes 1 and 3, and also between modes 2 and 4, when the measurements are noiseless, and therefore we present results from only modes 1 and 2 of estimation in Table I. For mode 1, the first observation is that there exist several estimates that deviate from the nominal values as shown on the first line. This is because in this case we choose the lowest-order polynomials defined by the coefficients of $\bar{Z}_1(s)$ and the resulting polynomial system has multiple solutions, among which the nominal set is only one of them. Second, as expected from the above observation that only even orders of δ_1 and ω_d enter the polynomial system, the signs of these parameters are indeterminate. In estimation mode 2, the estimate quality increases and, in fact, the only uncertainty is in the sign of δ_1 and ω_d. This is an example of how the choice of observable dictates the quality of the estimation.

In summary, we see that given noiseless measurement records, the above estimation algorithm can determine the unknown Hamiltonian and Lindblad parameters to within the limitations of the data (e.g., in the above example, the limitations were that ω_1, ω_2, γ_1, and γ_2 are not individually estimable and that the signs of δ_1 and ω_d are not estimable).

V. NOISY MEASUREMENTS

In this section we investigate the robustness of the system identification algorithm by reexamining the two-qubit dissipative energy transfer example with noisy measurement traces. In principle, the noise on expectation values of observables can be made arbitrarily small since the signal-to-noise decreases as $1/\sqrt{N}$, where N is the number of measurements that are averaged to estimate the expectation value of the observable. Because of this, measurement noise is especially small in ensemble systems like NMR [2]; however, in systems without natural access to ensembles, e.g., a single superconducting qubit, noise on time traces cannot be neglected in practical situations and we must assess the robustness of the above system identification algorithm to noise.

We consider the same system as in Sec. IV, with access to time traces of one or both observables: $\langle \sigma_z^1(t) \rangle$ and $\langle \sigma_z^2(t) \rangle$. Suppose that these time traces are corrupted by additive Gaussian noise

$$z_i^{\text{noisy}}(j) = \bar{z}_i(j) + \xi_i(j),$$

where $\xi_i(j) \sim \mathcal{N}(0, \sigma^2)$ for all i, j. Since the expectation values are formed by averaging many independent measurement outcomes, this is a reasonable model for the noise obtained by the central-limit theorem. We construct the Hankel matrix and perform the estimation in exactly the same way as in Sec. IV, with the only difference being that n_Σ is fixed to be 5 instead of the rank of the Hankel matrix $\mathbf{H}_{rs}(0)$, since the order of the denominator polynomial on the left-hand side of Eq. (18) [which takes the form in Eqs. (25) or (28) for this example] is 5.

To assess the quality of estimation, we compute the relative error in estimation for each of the seven parameters as

$$e_i = \left| \frac{\hat{\theta}_i - \theta_i}{\theta_i} \right| \times 100\%,$$

where θ_i and $\hat{\theta}_i$ are the nominal and estimated values of the parameter, respectively. If the estimation produces multiple solutions, then we choose the one with the least sum of errors $\sum_{i=1}^7 e_i$. We generate $M = 500$ instances of noise with given standard deviation σ, and calculate the estimation errors for each instance. These errors are then averaged to yield a mean relative error $\bar{e}_i$, which captures the performance of the algorithm. We evaluate these mean relative errors for standard deviations $\sigma = 0.05, 0.10, 0.15$, as well as for the noiseless case ($\sigma = 0$). The initial state in all instances is the same as in Sec. IV, and the only difference in parameters is that the duration of the measurement time traces is longer: $t_f = 120 \ \mu$s.

The first observation from this simulation (data not shown) is that there is a difference between modes 1 and 3 of estimation (and modes 2 and 4) when the measurements are noisy; it is beneficial to use data from both measurement time traces, $z_1^{\text{noisy}}(t)$ and $z_2^{\text{noisy}}(t)$, to form the realization even if the polynomial system is formed from the Laplace transform of one of the time traces. Therefore we present only the estimation modes 3 and 4.

Figure 2 shows the mean relative error for each parameter as a function of the standard deviation of the measurement noise. The left (right) column plots $\bar{e}_i$ under mode 3 (mode 4) of estimation. This figure shows that the average error in estimation is small for small σ, but quickly becomes quite large. An interesting feature is that the performance can be very different under mode 3 and mode 4 of estimation, with one performing better for some parameters and worse for others. Also, the performance can vary significantly among
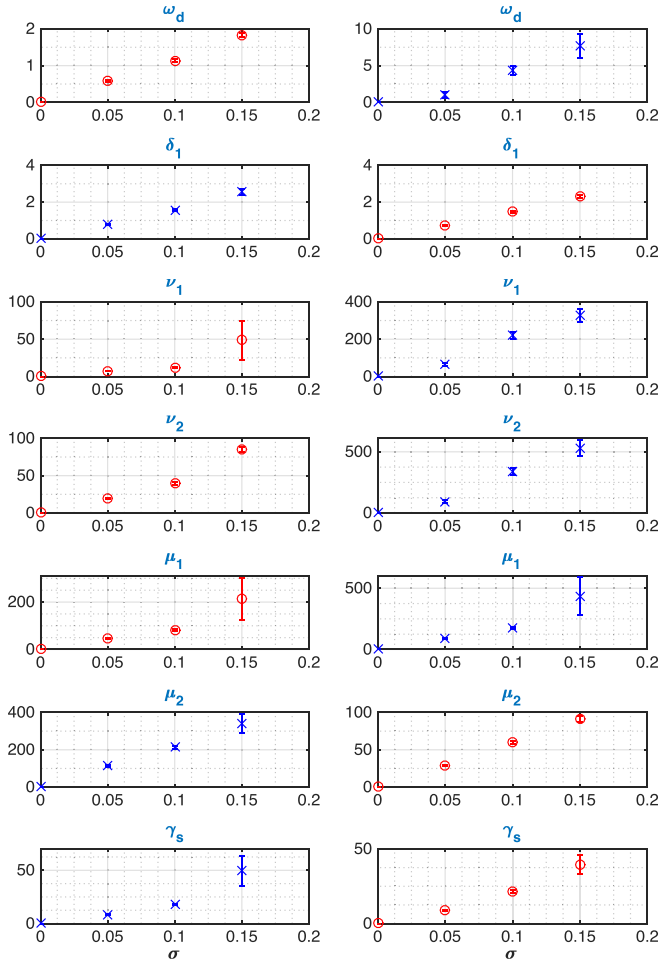
FIG. 2. (Color online) Average relative error of parameter estimates as a function of the standard deviation (σ) of the additive noise on the measurement traces. In all the plots, the y axis shows the relative error as a percentage and the x axis is σ. The left (right) column shows the error for estimation under mode 3 (mode 4). The red circles denote the result of the better estimation mode for that parameter (lower maximum error), and the error bars indicate the standard error for the average (which is taken over $M = 500$ instances of noise).

parameters. Estimates of the Hamiltonian parameters ω_d and δ_1 exhibit the greatest robustness to measurement noise, while estimates of the open-system parameters are more sensitive. In particular, estimates of μ_1, μ_2, and ν_2, which are the parameters of smallest magnitude, suffer the most from measurement noise. It is clear that this open-system identification algorithm is not as robust as the Hamiltonian version [1]. However, in the regions of low noise ($\sigma < 0.1$) relevant for NMR and other ensemble experimental platforms, the performance is acceptable, especially for the Hamiltonian parameters, which can be estimated well even in the presence of dissipation and dephasing.

VI. DISCUSSION

We have extended the quantum system identification approach developed in Ref. [1] for Hamiltonian systems to Markovian open quantum systems. The approach proceeds by forming a realization of the quantum system from (time-dependent) input-output data and then uses this realization to form a system of polynomial equations for the parameters that define the system. The strengths of the approach are its ability to incorporate prior information and its ability to produce parameter estimates even with time-dependent measurements of only a few observables.

As with the Hamiltonian case dealt with in Ref. [1], having access to time-dependent data enables us to directly estimate the generator of dynamics, which has a significant advantage in that it is specified by fewer parameters than the dynamical map at a fixed time (e.g., a Kraus map or unitary). In contrast to the Hamiltonian case, the Markovian open-system identification scenario ideally requires the symbolic computation of a resolvent as expressed in Eq. (18), which can be computationally expensive for large systems. Alternatively, as mentioned in Sec. III B one could avoid the resolvent computation by using a power-series expansion of the resolvent. This approach is equivalent to using the Markov parameters of an LTI system as the model realization invariant, as opposed to the Laplace transform of the output. Although this is computationally advantageous, we have found that the Markov parameters are more susceptible to measurement noise and therefore this approach is expected to yield less robust estimates of the parameters. As a consequence, we expect that symbolic computation of the resolvent will be the fundamental limitation to applying this approach to identification of large Markovian open quantum systems. However, as demonstrated in Appendix and Sec. IV, the required symbolic computation can be easily performed for small open systems, which are still difficult to identify using other approaches.

The noise robustness results in Sec. V suggest that a direction for future work is to understand exactly why this realization-based system identification algorithm is more robust to measurement noise in the Hamiltonian (closed-system) case than in the open-system case. One clue as to why this may be is that Markovian open-system parameters almost always dictate exponential rates of decay of measurement traces, and parameter fitting to decaying exponentials is a notoriously ill-conditioned problem [28]. More work is required to understand the properties of this algorithm under measurement noise and to increase its robustness in the open-system scenario.

APPENDIX: CASE STUDIES

In this appendix we present some examples that illustrate the Markovian open-system identification algorithm

developed in this paper. The system studied in all examples is a 1D chain of n qubits, with closed-system dynamics governed by the Hamiltonian

$$H = \sum_{k=1}^{n} \frac{\omega_k}{2}\sigma_z^k + \sum_{k=1}^{n-1} \delta_k(\sigma_+^k\sigma_-^{k+1} + \sigma_-^k\sigma_+^{k+1}). \qquad (A1)$$

This Hamiltonian is often used as a model for a spin "wire" that enables quantum state transfer [29], and is relevant to resonant energy transfer mechanisms between atomic or solid-state systems; e.g., [30].

In Ref. [1] we analyzed the identification of the Hamiltonian parameters of this closed system when the observable being directly measured is $\langle\sigma_x^1\rangle$. When the generalized Pauli operators is chosen as the basis of operators $\{F_k\}$, the accessible set was found to be $\bar{G} = \{2^{-n/2}\sigma_x^1, 2^{-n/2}\sigma_y^1\} \cup \{2^{-n/2}\sigma_z^1\cdots\sigma_z^{k-1}\sigma_x^k, 2^{-n/2}\sigma_z^1\cdots\sigma_z^{k-1}\sigma_y^k\}_{k=2}^n$. Then denoting the average of the observables in $\bar{G}$ as $\mathbf{x}_a = [\bar{x}_1, \bar{y}_1, \ldots, \bar{x}_n, \bar{y}_n]^T$, where $\bar{x}_1 = \langle\sigma_x^1\rangle$, $\bar{y}_1 = \langle\sigma_y^1\rangle$ and $\bar{x}_k = \langle\sigma_z^1\cdots\sigma_z^{k-1}\sigma_x^k\rangle$, $\bar{y}_k = \langle\sigma_z^1\cdots\sigma_z^{k-1}\sigma_y^k\rangle$ for $k \geq 2$, the dynamics of $\mathbf{x}_a$ is determined by

$$\dot{\mathbf{x}}_a = \tilde{\mathbf{A}}\mathbf{x}_a, \qquad (A2)$$

where the system matrix $\tilde{\mathbf{A}}$ is given by [1]:

$$\tilde{\mathbf{A}} = \begin{bmatrix} 0 & \omega_1 & 0 & -\delta_1 & & & & \\ -\omega_1 & 0 & \delta_1 & 0 & 0 & & & \\ 0 & -\delta_1 & 0 & \omega_2 & 0 & \ddots & & \\ \delta_1 & 0 & -\omega_2 & 0 & \ddots & \ddots & 0 & \\ 0 & \ddots & \ddots & \ddots & \ddots & \ddots & & -\delta_{n-1} \\ & \ddots & \ddots & \ddots & 0 & \delta_{n-1} & 0 & \\ & & 0 & 0 & -\delta_{n-1} & 0 & \omega_n \\ & & & \delta_{n-1} & 0 & -\omega_n & 0 \end{bmatrix}. \qquad (A3)$$

Finally, in this basis the direct observation of $\langle\sigma_x^1\rangle$ corresponds to $\mathbf{c} = [1,0,0,\ldots,0]$.

In the following we will consider various types of open-system dynamics for this 1D spin chain and apply the algorithm developed above to estimate the parameters defining the Hamiltonian and the open-system dynamics.

1. Independent dephasing

We first consider a common decoherence model for spin-$\frac{1}{2}$ systems, namely, independent Markovian dephasing on each spin [26]. This is described by the Lindblad terms

$$\sum_{k=1}^{n} 2\gamma_k\left(\sigma_z^k\rho\sigma_z^k - \rho\right), \qquad (A4)$$

where the superscript k indexes the spin, and the factor 2 is for ease of expression. Comparing Eqs. (3) and (A4), we see that the independent dephasing model is equivalent to the choice

$$g_{lk} = \begin{cases} \gamma_k\delta_{lk} & \text{if } \operatorname{tr}\left(X_k\sigma_z^k\right) \neq 0, \\ 0 & \text{otherwise}, \end{cases} \qquad (A5)$$

meaning that the Lindblad coefficient matrix $\mathbf{G}$ is diagonal and real. Again, assuming that the directly measured quantity is $\langle\sigma_x^1\rangle$, the system matrix $\tilde{\mathbf{A}}$ now becomes

$$\tilde{\mathbf{A}} = \begin{bmatrix} -\gamma_1 & \omega_1 & 0 & -\delta_1 & & & & \\ -\omega_1 & -\gamma_1 & \delta_1 & 0 & 0 & & & \\ 0 & -\delta_1 & -\gamma_2 & \omega_2 & 0 & \ddots & & \\ \delta_1 & 0 & -\omega_2 & -\gamma_2 & \ddots & \ddots & 0 & \\ 0 & \ddots & \ddots & \ddots & \ddots & \ddots & & -\delta_{n-1} \\ & \ddots & \ddots & \ddots & -\gamma_{n-1} & \delta_{n-1} & 0 & \\ & & 0 & 0 & -\delta_{n-1} & -\gamma_n & \omega_n \\ & & & \delta_{n-1} & 0 & -\omega_n & -\gamma_n \end{bmatrix}. \qquad (A6)$$

Comparing Eqs. (A3) and (A6), we observe that the dephasing terms introduce nonzero diagonal elements in $\tilde{\mathbf{A}}$, whereas the accessible set $\bar{G}$ remains the same. In addition, for these dynamics, $\tilde{\mathbf{b}} = \mathbf{0}$. All parameters in the Hamiltonian Eq. (A1) and Lindblad coefficients in Eq. (A4) appear in $\tilde{\mathbf{A}}$, and therefore it is possible to identify these parameters by measuring $\langle \sigma_x^1 \rangle$.

Consider the case of three-qubit ($n = 3$), whereby

$$\tilde{\mathbf{A}} = \begin{bmatrix} -\gamma_1 & \omega_1 & 0 & -\delta_1 & 0 & 0 \\ -\omega_1 & -\gamma_1 & \delta_1 & 0 & 0 & 0 \\ 0 & -\delta_1 & -\gamma_2 & \omega_2 & 0 & -\delta_2 \\ \delta_1 & 0 & -\omega_2 & -\gamma_2 & \delta_2 & 0 \\ 0 & 0 & 0 & -\delta_2 & -\gamma_3 & \omega_3 \\ 0 & 0 & \delta_2 & 0 & -\omega_3 & -\gamma_3 \end{bmatrix}. \tag{A7}$$

Now, if the initial state is given by $|\psi(0)\rangle = (|0\rangle + |1\rangle)/\sqrt{2} \otimes |00\rangle$, then we have

$$\mathbf{x}_a(0) = [1, \quad 0, \quad 0, \quad 0, \quad 0, \quad 0]^\mathsf{T}. \tag{A8}$$

This is an example where the Laplace transform of the measurement trace $\bar{x}_1(t)$ takes the canonical form given by Eq. (19), and we obtain

$$\bar{X}_1(s) = \frac{s^5 + q_4 s^4 + q_3 s^3 + q_2 s^2 + q_1 s + q_0}{s^6 + p_5 s^5 + p_4 s^4 + p_3 s^3 + p_2 s^2 + p_1 s + p_0},$$

where the expressions for p_k and q_k in terms of Hamiltonian parameters and Lindblad coefficients are

$$p_5 = 2(\gamma_1 + \gamma_2 + \gamma_3),$$
$$p_4 = 2\delta_1^2 + 2\delta_2^2 + \gamma_1^2 + 4\gamma_1\gamma_2 + \gamma_2^2 + 4(\gamma_1 + \gamma_2)\gamma_3 + \gamma_3^2 + \omega_1^2 + \omega_2^2 + \omega_3^2,$$
$$p_3 = 2\big[\gamma_1^2\gamma_2 + \gamma_1\gamma_2^2 + \gamma_1^2\gamma_3 + 4\gamma_1\gamma_2\gamma_3 + \gamma_2^2\gamma_3 + \gamma_1\gamma_3^2 + \gamma_2\gamma_3^2 + \delta_2^2(2\gamma_1 + \gamma_2 + \gamma_3) + \delta_1^2(\gamma_1 + \gamma_2 + 2\gamma_3)$$
$$\quad + \gamma_2\omega_1^2 + \gamma_3\omega_1^2 + \gamma_1\omega_2^2 + \gamma_3\omega_2^2 + (\gamma_1 + \gamma_2)\omega_3^2\big],$$
$$p_2 = \delta_1^4 + \delta_2^4 + \gamma_1^2\gamma_2^2 + 4\gamma_1^2\gamma_2\gamma_3 + 4\gamma_1\gamma_2^2\gamma_3 + \gamma_1^2\gamma_3^2 + 4\gamma_1\gamma_2\gamma_3^2 + \gamma_2^2\gamma_3^2 + \gamma_2^2\omega_1^2 + 4\gamma_2\gamma_3\omega_1^2 + \gamma_3^2\omega_1^2 + \gamma_1^2\omega_2^2 + 4\gamma_1\gamma_3\omega_2^2$$
$$\quad + \gamma_3^2\omega_2^2 + \omega_1^2\omega_2^2 + \big(\gamma_1^2 + 4\gamma_1\gamma_2 + \gamma_2^2 + \omega_1^2 + \omega_2^2\big)\omega_3^2 + 2\delta_2^2\big[\gamma_1^2 + \gamma_2\gamma_3 + 2\gamma_1(\gamma_2 + \gamma_3) + \omega_1^2 - \omega_2\omega_3\big]$$
$$\quad + 2\delta_1^2\big[\delta_2^2 + \gamma_1\gamma_2 + 2(\gamma_1 + \gamma_2)\gamma_3 + \gamma_3^2 - \omega_1\omega_2 + \omega_3^2\big],$$
$$p_1 = 2\big(\delta_2^4\gamma_1 + \delta_1^4\gamma_3 + \gamma_2\gamma_3\big[\gamma_1\gamma_2\gamma_3 + \gamma_1^2(\gamma_2 + \gamma_3) + (\gamma_2 + \gamma_3)\omega_1^2\big] + \gamma_3\big[\gamma_1(\gamma_1 + \gamma_3) + \omega_1^2\big]\omega_2^2$$
$$\quad + \big\{\gamma_2\big[\gamma_1(\gamma_1 + \gamma_2) + \omega_1^2\big] + \gamma_1\omega_2^2\big\}\omega_3^2 + \delta_1^2\big\{\delta_2^2(\gamma_1 + \gamma_3) + \gamma_3\big[2\gamma_1\gamma_2 + (\gamma_1 + \gamma_2)\gamma_3 - 2\omega_1\omega_2\big]$$
$$\quad + (\gamma_1 + \gamma_2)\omega_3^2\big\} + \delta_2^2\big[\gamma_1^2(\gamma_2 + \gamma_3) + (\gamma_2 + \gamma_3)\omega_1^2 + 2\gamma_1(\gamma_2\gamma_3 - \omega_2\omega_3)\big]\big),$$
$$p_0 = \big[\delta_1^4 + 2\delta_1^2(\gamma_1\gamma_2 - \omega_1\omega_2) + \big(\gamma_1^2 + \omega_1^2\big)\big(\gamma_2^2 + \omega_2^2\big)\big]\big(\gamma_3^2 + \omega_3^2\big) + 2\delta_2^2\big[\delta_1^2(\gamma_1\gamma_3 + \omega_1\omega_3) + \delta_2^4(\gamma_1^2 + \omega_1^2)$$
$$\quad + \big(\gamma_1^2 + \omega_1^2\big)(\gamma_2\gamma_3 - \omega_2\omega_3)\big],$$

and

$$q_4 = \gamma_1 + 2\gamma_2 + 2\gamma_3,$$
$$q_3 = \delta_1^2 + 2\delta_2^2 + \gamma_2^2 + 4\gamma_2\gamma_3 + \gamma_3^2 + 2\gamma_1(\gamma_2 + \gamma_3) + \omega_2^2 + \omega_3^2,$$
$$q_2 = 2\delta_2^2(\gamma_1 + \gamma_2 + \gamma_3) + \delta_1^2(\gamma_2 + 2\gamma_3) + 2\gamma_3\big(\gamma_2(\gamma_2 + \gamma_3) + \omega_2^2\big) + 2\gamma_2\omega_3^2 + \gamma_1\big(\gamma_2^2 + 4\gamma_2\gamma_3 + \gamma_3^2 + \omega_2^2 + \omega_3^2\big),$$
$$q_1 = \delta_2^4 + \gamma_2\gamma_3[\gamma_2\gamma_3 + 2\gamma_1(\gamma_2 + \gamma_3)] + \gamma_3(2\gamma_1 + \gamma_3)\omega_2^2 + \big(2\gamma_1\gamma_2 + \gamma_2^2 + \omega_2^2\big)\omega_3^2 + 2\delta_2^2[\gamma_2\gamma_3 + \gamma_1(\gamma_2 + \gamma_3) - \omega_2\omega_3]$$
$$\quad + \delta_1^2\big(\delta_2^2 + 2\gamma_2\gamma_3 + \gamma_3^2 + \omega_3^2\big),$$
$$q_0 = \delta_2^4\gamma_1 + \delta_2^2\big(\delta_1^2\gamma_3 + 2\gamma_1\gamma_2\gamma_3 - 2\gamma_1\omega_2\omega_3\big) + \big[\delta_1^2\gamma_2 + \gamma_1\big(\gamma_2^2 + \omega_2^2\big)\big]\big(\gamma_3^2 + \omega_3^2\big).$$

The Hamiltonian and Lindblad parameters can be obtained by solving these polynomial equations.

2. Independent relaxation

Next we consider another common form of Markovian decoherence, i.e., independent relaxation [26]. This amounts to the following Lindblad terms:

$$\sum_k 2g_k^- \left(\sigma_-^k \rho \sigma_+^k - \frac{1}{2}\sigma_+^k \sigma_-^k \rho - \frac{1}{2}\rho \sigma_+^k \sigma_-^k \right), \tag{A9}$$

where g_k^- is the relaxation rate of qubit k.

Consider for example, the two-qubit case where we directly observe $\langle \sigma_x^1 \rangle$. Performing the generalized filtration procedure prescribed by Eq. (13), the accessible portion of the coherence vector is found to be $\mathbf{x}_a = [\langle \sigma_x^1 \rangle, \langle \sigma_y^1 \rangle, \langle \sigma_x^2 \rangle, \langle \sigma_y^2 \rangle, \langle \sigma_x^1 \sigma_z^1 \rangle, \langle \sigma_y^1 \sigma_z^1 \rangle, \langle \sigma_z^1 \sigma_x^2 \rangle, \langle \sigma_z^1 \sigma_y^2 \rangle]^{\mathsf{T}}$. Comparing with Eq. (A2), we see that the Lindblad relaxation term has introduced four new elements into the accessible state vector, namely, $\langle \sigma_x^2 \rangle$, $\langle \sigma_y^2 \rangle$, $\langle \sigma_x^1 \sigma_z^1 \rangle$, and $\langle \sigma_y^1 \sigma_z^1 \rangle$. The dynamical equation is described by Eq. (14), with

$$\tilde{\mathbf{A}} = \begin{bmatrix} -g_1^- & \omega_1 & 0 & 0 & 0 & 0 & 0 & -\delta_1 \\ -\omega_1 & -g_1^- & 0 & 0 & 0 & 0 & \delta_1 & 0 \\ 0 & 0 & -g_2^- & \omega_2 & 0 & -\delta_1 & 0 & 0 \\ 0 & 0 & -\omega_2 & -g_2^- & \delta_1 & 0 & 0 & 0 \\ -2g_2^- & 0 & 0 & -\delta_1 & -2g_2^- - g_1^- & \omega_1 & 0 & 0 \\ 0 & -2g_2^- & \delta_1 & 0 & -\omega_1 & -2g_2^- - g_1^- & 0 & 0 \\ 0 & -\delta_1 & -2g_1^- & 0 & 0 & 0 & -2g_1^- - g_2^- & \omega_2 \\ \delta_1 & 0 & 0 & -2g_1^- & 0 & 0 & -\omega_2 & -2g_1^- - g_2^- \end{bmatrix}, \tag{A10}$$

and $\tilde{\mathbf{b}} = \mathbf{0}$. Note that the constant forcing vector $\tilde{\mathbf{b}}$ for the dynamics of the accessible set can be zero even if $\mathbf{b} \neq 0$ (as in this case).

Suppose we prepare the initial state $|\psi(0)\rangle = (|0\rangle + |1\rangle)/\sqrt{2} \otimes |0\rangle$; then

$$\mathbf{x}_a(0) = [1, \quad 0, \quad 0, \quad 0, \quad 1, \quad 0, \quad 0, \quad 0]^{\mathsf{T}}.$$

The resolvent on the left-hand side of Eq. (18) can be computed symbolically in this case, and consequently the Laplace transform of the measurement trace $\bar{x}_1$ is

$$\bar{X}_1(s) = \frac{s^7 + q_6 s^6 + \cdots + q_1 s + q_0}{s^8 + p_7 s^7 + p_6 s^6 + \cdots + p_1 s + p_0}. \tag{A11}$$

The expressions for the coefficients in Eq. (A11) are quite involved and so we present only the most concise ones here:

$$q_6 = 7g_1^- + 8g_2^-, \quad q_5 = 26(g_2^-)^2 + 48g_2^- g_1^- + 3\delta_1^2 + 2\omega_2^2 + 19(g_1^-)^2 + \omega_1^2,$$

$$q_4 = 130g_1^- (g_2^-)^2 + 17\delta_1^2 g_2^- + 5\omega_1^2 g_1^- + 10\omega_2^2 g_1^- + 12\omega_2^2 g_2^- + 108(g_1^-)^2 g_2^- + 44(g_2^-)^3 + 18\delta_1^2 g_1^- + 25(g_1^-)^3 + 4\omega_1^2 g_2^-,$$

and

$$p_7 = 8g_1^- + 8g_2^-, \quad p_6 = 2\omega_2^2 + 26(g_1^-)^2 + 26(g_2^-)^2 + 56g_2^- g_1^- + 2\omega_1^2 + 4\delta_1^2. \tag{A12}$$

These five equations and the realization formed from the measurement data can be used to solve for the five unknown parameters in this model.

To treat a case where $\tilde{\mathbf{b}} \neq 0$, we now alter the setup to consider direct measurement of a time trace of $\bar{z}_1 \equiv \langle \sigma_z^1 \rangle$. In this case, with the Hamiltonian given in Eq. (A1) with $n = 2$ and independent relaxation as prescribed in Eq. (A9), the accessible set becomes $\bar{G} = \{\sigma_z^1, \sigma_z^2, \sigma_x^1 \sigma_x^2, \sigma_x^1 \sigma_y^1, \sigma_y^1 \sigma_x^2, \sigma_y^1 \sigma_y^2\}$. The dynamics of $\mathbf{x}_a$ is determined by Eq. (14) with

$$\tilde{\mathbf{A}} = \begin{bmatrix} -2g_1^- & 0 & 0 & \delta_1 & -\delta_1 & 0 \\ 0 & -2g_2^- & 0 & -\delta_1 & \delta_1 & 0 \\ 0 & 0 & -g_s^- & \omega_2 & \omega_1 & 0 \\ -\delta_1 & \delta_1 & -\omega_2 & -g_s^- & 0 & \omega_1 \\ \delta_1 & -\delta_1 & -\omega_1 & 0 & -g_s^- & \omega_2 \\ 0 & 0 & 0 & -\omega_1 & -\omega_2 & -g_s^- \end{bmatrix},$$

$$\tilde{\mathbf{b}} = [-g_1^-, \quad -g_2^-, \quad 0, \quad 0, \quad 0, \quad 0]^{\mathsf{T}},$$

where $g_s^- = g_1^- + g_2^-$. In this basis $\mathbf{c} = [1,0,0,0,0,0]$. Let the initial state be $|\psi(0)\rangle = (|0\rangle + |1\rangle)/\sqrt{2} \otimes |0\rangle$ as before, in which case

$$\mathbf{x}_a(0) = [0, \quad 1, \quad 0, \quad 0, \quad 0, \quad 0]^{\mathsf{T}}.$$

Again, we can symbolically calculate the resolvents in this case and obtain the Laplace transform of the measurement trace $\bar{z}_1$ as

$$\bar{Z}_1(s) = \mathbf{c}(s\mathbf{I} - \mathbf{A})^{-1}\mathbf{x}_a(0) + \mathbf{c}(s\mathbf{I} - \mathbf{A})^{-1}\mathbf{b}/s = \frac{q_3 s^3 + q_2 s^2 + q_1 s + q_0}{s^5 + p_4 s^4 + p_3 s^3 + p_2 s^2 + p_1 s}, \tag{A13}$$

with

$$q_3 = -g_1^-, \quad q_2 = 2\delta_1^2 - 2(g_1^-)^2 - 4g_1^- g_2^-, \quad q_1 = -g_1^-\left[(g_1^-)^2 + 6g_1^- g_2^- + 5(g_2^-)^2 + \omega_d^2\right],$$
$$q_0 = -2\delta_1^2(g_1^- + g_2^-)^2 - 2g_1^- g_2^-\left[(g_1^- + g_2^-)^2 + \omega_d^2\right], \tag{A14}$$

and

$$p_4 = 4(g_1^- + g_2^-), \quad p_3 = 4\delta_1^2 + 5(g_1^-)^2 + 14g_1^- g_2^- + 5(g_2^-)^2 + \omega_d^2, \quad p_2 = 2(g_1^- + g_2^-)\left[4\delta_1^2 + (g_1^-)^2 + 6g_1^- g_2^- + (g_2^-)^2 + \omega_d^2\right],$$
$$p_1 = 4\delta_1^2(g_1^- + g_2^-)^2 + 4g_1^- g_2^-\left[(g_1^- + g_2^-)^2 + \omega_d^2\right], \tag{A15}$$

where $\omega_d = \omega_1 - \omega_2$. An interesting aspect of this example is that from Eqs. (A14) and (A15) we can identify g_1^-, g_2^-, and δ_1, but only $\omega_1 - \omega_2$. The individual transition energies of the qubits do not influence the measurement trace, and only the their difference does.

---

[1] J. Zhang and M. Sarovar, Phys. Rev. Lett. **113**, 080401 (2014).

[2] S. Y. Hou, H. Li, and G. L. Long, arXiv:1410.3940.

[3] C. P. Slichter, *Principles of Magnetic Resonance*, 3rd ed. (Springer, Berlin, 1996).

[4] A. Smith, C. A. Riofrío, B. E. Anderson, H. Sosa-Martinez, I. H. Deutsch, and P. S. Jessen, Phys. Rev. A **87**, 030102(R) (2013).

[5] C. C. Gerry and P. L. Knight, *Introductory Quantum Optics* (Cambridge University Press, New York, 2005).

[6] N. Boulant, T. F. Havel, M. A. Pravia, and D. G. Cory, Phys. Rev. A **67**, 042322 (2003).

[7] J. H. Cole, S. G. Schirmer, A. D. Greentree, C. J. Wellard, D. K. L. Oi, and L. C. L. Hollenberg, Phys. Rev. A **71**, 062312 (2005).

[8] S. J. Devitt, J. H. Cole, and L. C. L. Hollenberg, Phys. Rev. A **73**, 052317 (2006).

[9] D. Burgarth, K. Maruyama, and F. Nori, Phys. Rev. A **79**, 020305 (2009).

[10] D. Burgarth and K. Maruyama, New J. Phys. **11**, 103019 (2009).

[11] C. Di Franco, M. Paternostro, and M. S. Kim, Phys. Rev. Lett. **102**, 187203 (2009).

[12] B. Bellomo, A. De Pasquale, G. Gualdi, and U. Marzolino, Phys. Rev. A **82**, 062104 (2010).

[13] B. Bellomo, A. De Pasquale, G. Gualdi, and U. Marzolino, J. Phys. A: Math. Theor. **43**, 395303 (2010).

[14] C. E. Granade, C. Ferrie, N. Wiebe, and D. G. Cory, New J. Phys. **14**, 103013 (2012).

[15] S. G. Schirmer, D. K. L. Oi, W. Zhou, E. Gong, and M. Zhang, arXiv:1205.6220.

[16] Y. Kato and N. Yamamoto, New J. Phys. **16**, 023024 (2014).

[17] J. M. Dominy, L. C. Venuti, A. Shabani, and D. A. Lidar, arXiv:1312.0973v1.

[18] V. Jagadish and A. Shaji, arXiv:1401.1058v1.

[19] K. Lendi, J. Phys. A: Math. Theor. **20**, 15 (1987).

[20] R. Alicki and K. Lendi, *Quantum Dynamical Semigroups and Applications*, Lecture Notes in Physics Vol. 717 (Springer, Berlin, 2007).

[21] S. Sastry, *Nonlinear Systems* (Springer, New York, 1999).

[22] F. M. Callier and C. A. Desoer, *Linear System Theory* (Springer, New York, 1991).

[23] J. N. Juang and R. S. Pappa, J. Guid. Control. Dyn. **8**, 620 (1985).

[24] G. F. Franklin, J. D. Powell, and M. L. Workman, *Digital Control of Dynamic Systems* (Addison-Wesley, Boston, 1997).

[25] D. Burgarth and K. Yuasa, Phys. Rev. Lett. **108**, 080502 (2012).

[26] H.-P. Breuer and F. Petruccione, *The Theory of Open Quantum Systems* (Oxford University Press, Oxford, 2002).

[27] Y. Guan and J. Verschelde, *PHClab: A MATLAB/Octave Interface to PHCpack*, IMA Software for Algebra and Geometry Vol. 148 (Springer-Verlag, Berlin, 2008).

[28] *Exponential Data Fitting and its Applications*, edited by V. Pereyra and G. Scherer (Bentham Science, 2010).

[29] S. Bose, Contemp. Phys. **48**, 13 (2007).

[30] I. I. Ryabtsev, D. B. Tretyakov, I. I. Beterov, and V. M. Entin, Phys. Rev. Lett. **104**, 073003 (2010).